Contraction of random actomyosin arrays is enabled by the combined effect of actin treadmilling and crosslinking *Supporting Material*

Dietmar B. Oelz[1], Boris Y. Rubinstein[2], Alex Mogilner[1,3].

[1]Courant Inst. of Math. Sciences, New York University, New York, NY, USA

[2]Stowers Institute, Kansas City, MO, USA

[3]Department of Biology, New York University, New York, NY, USA .

S1 Mathematical Model

S1.1 Numerical simulations:

We initialize the simulations by generating a random ring configuration specifying the radius and $N+M$ random angular positions of filaments and clusters. The polarities of filaments are also chosen randomly. We solve the model equations

$$-\sum_k \vartheta_{ik}\, F_s\left(n_i - \frac{v_i - V_k}{V_m}\right) + \sum_j \eta\, A_{ij}\,(v_i - v_j) \;=\; 0\,, \quad i = 1\dots N \tag{1}$$

$$\sum_i \vartheta_{ik}\, F_s\left(n_i - \frac{v_i - V_k}{V_m}\right) \;=\; 0\,, \quad k = 1\dots M \tag{2}$$

$$-\sum_{i,k} \vartheta_{ik}\, F_s \bar{\tau}_{ik}\left(n_i - \frac{v_i - V_k}{V_m}\right) + \frac{1}{2}\sum_{i,j} \eta\, A_{ij}\tau_{ij}\,(v_i - v_j) \;=\; \sigma\,. \tag{3}$$

under two conditions. The first condition is isometric, corresponding to the fixed, unchanging radius $R =$ const. In this case, we solve the system Eq. 1 and Eq. 2 for a given R, and then use Eq. 3 to compute the isometric stress σ. Alternatively, we examine the ring contracting against zero pressure, so $\sigma = 0$. In this case, we solve the whole system Eq. 1-Eq. 3, where in Eq. 3 the right hand side is zero, and thus compute the evolution of the radius $R(t)$ and respective contraction rate $\dot{R}$. These two cases completely determine the system behavior in more complex conditions due to the linear force-velocity relation in the general system.

We simulate the system Eq. 1-Eq. 3 of ordinary differential equations using a time implicit discretization and functional minimization method, as illustrated in the Supporting Material. At each step, we alternate the simulation of movements with the simulation of treadmilling of actin and binding/unbinding of myosin. Actin treadmilling and myosin kinetics events are simulated at each computational step according to the rules described in the Model section. In the simulation, we use the reference set of parameter values summarized in Table S1 in the Supporting Material, and vary these parameters to investigate dependence of contractility on the parameters. Relevance of the parameter values to various experimental systems is analyzed in Discussion.

S1.2 The simplest model for 2 filaments

To build intuition, consider the simplest possible model of a contractile system consisting of only two anti-parallel actin filaments, s, one myosin cluster, and crosslinking friction between two filament overlaps (Fig. S1 A).

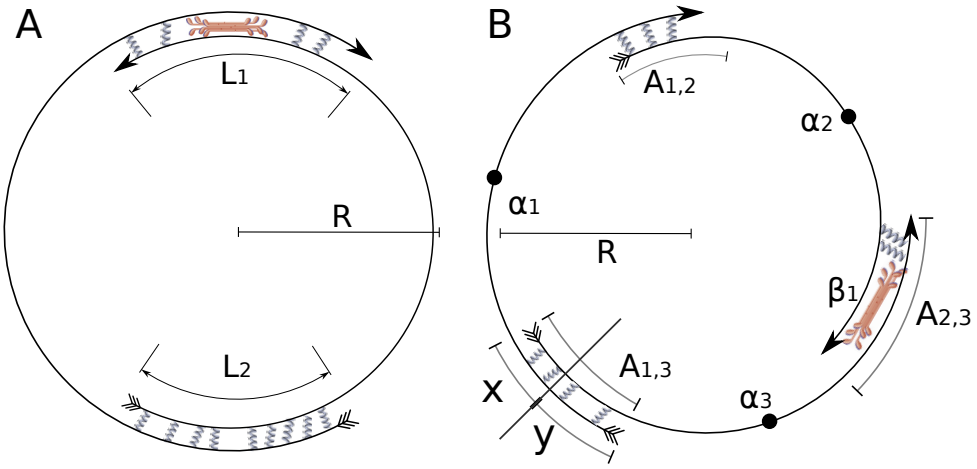

Figure S1: A: Schematic representation of a minimal contractile ring with two anti-parallel actin filaments and myosin located at the overlap of the pointed end sections. B: Minimal contractile ring consisting of three filaments and one myosin cluster. Notations are discussed in the text.

The angular positions of the center points of the two actin filaments are $\alpha_1 = \alpha_1(t)$ and $\alpha_2 = \alpha_2(t)$. The two actin filaments are anti-parallel; $n_1 = 1$ and $n_2 = -1$. In this scenario, the two filaments overlap twice, in a region of length L_1 limited by their pointed ends, where also the myosin cluster is located, and in a region of length L_2, on the opposite side of the ring, limited by their barbed ends. Myosin is biased to the pointed ends to illustrate the effective contraction.

Let $d(a,b) = mod(a-b, 2\pi) \in [0, 2\pi)$ denote the difference between angles measured in the clockwise direction, and observe that $d(a,b)+d(b,a) = 2\pi$. The size of timesteps is denoted by Δt and $n = 0, 1, 2, ...$ is the index referring to the sequence of discrete times $0, \Delta t, 2\Delta t, ...$ A simple set of initial data is $R^0 = 1$, $\alpha_1^0 = 0$, $\alpha_2^0 = \pi$, the lengths of the two filaments are $3\pi/2$ and we assume that one myosin cluster is located in the bundle at angle $\pi/2$. As the evolution of α_1 and α_2 is symmetric and since the myosin cluster moves with the average speed of the two actin filaments it is connected to, the cluster will remain at the exact center point between these two filaments at $\pi/2$.

Using the steepest descent approximation, where, given the past data α_1^n and α_2^n and R^n, we set

$$(\alpha_1^{n+1}, \alpha_2^{n+1}, R^{n+1}) = \text{argmin } U^n[\alpha_1, \alpha_2, R]$$

where

$$U[\alpha_1,\alpha_2,R] := F_s\left(R\,d(\alpha_2,\alpha_1) + \frac{(R\,d(\alpha_2,\alpha_1) - R^n\,d(\alpha_2^n,\alpha_1^n))^2}{2\Delta t V_m}\right) + \\ + \eta L_1 \frac{(R\,d(\alpha_2,\alpha_1) - R^n\,d(\alpha_2^n,\alpha_1^n))^2}{2\Delta t} + \eta L_2 \frac{(R\,d(\alpha_1,\alpha_2) - R^n\,d(\alpha_1^n,\alpha_2^n))^2}{2\Delta t} - \sigma 2\pi R.$$

The variation reads:

$$\delta U[\alpha_1,\alpha_2,R] = F_s\Big(R(\delta\alpha_2 - \delta\alpha_1) + \delta R\,d(\alpha_2,\alpha_1) + \\ + \frac{(R\,d(\alpha_2,\alpha_1) - R^n\,d(\alpha_2^n,\alpha_1^n))}{\Delta t V_m}(R(\delta\alpha_2 - \delta\alpha_1) + \delta R\,d(\alpha_2,\alpha_1))\Big) + \\ + \eta L_1 \frac{(R\,d(\alpha_2,\alpha_1) - R^n\,d(\alpha_2^n,\alpha_1^n))}{\Delta t}(R(\delta\alpha_2 - \delta\alpha_1) + \delta R\,d(\alpha_2,\alpha_1)) + \\ + \eta L_2 \frac{(R\,d(\alpha_1,\alpha_2) - R^n\,d(\alpha_1^n,\alpha_2^n))}{\Delta t}(R(\delta\alpha_1 - \delta\alpha_2) + \delta R\,d(\alpha_1,\alpha_2)) - \sigma\,2\pi\,\delta R\,.$$

We obtain the variational equations by collecting the coefficients of $\delta\alpha_1$, $\delta\alpha_2$ and δR and setting them to zero. The variational equation resulting from the variation of α_2 differs from the one obtained by varying α_1 only by its sign. Actually, the system is underdetermined due to the fact that we didn't define any interaction with the environment, and so at any time the system can be rotated freely around its axis.

We let formally $\Delta t \to 0$, so e.g. $(\alpha_1^{n+1} - \alpha_1^n)/\Delta t \to \dot{\alpha}_1$, and we use the following notations: $u_1 = \dot{R}\, d(\alpha_2, \alpha_1) + R(\dot{\alpha}_2 - \dot{\alpha}_1)$ and $u_2 = \dot{R}\, d(\alpha_1, \alpha_2) + R(\dot{\alpha}_1 - \dot{\alpha}_2)$, which satisfy $u_1 + u_2 = 2\pi\dot{R}$. We obtain the system:

$$0 = -F_s \left(1 + \frac{u_1}{V_m}\right) - \eta L_1\, u_1 + \eta L_2\, u_2 \tag{4}$$

$$0 = d(\alpha_2, \alpha_1) F_s \left(1 + \frac{u_1}{V_m}\right) + d(\alpha_2, \alpha_1)\eta L_1\, u_1 + d(\alpha_1, \alpha_2)\eta L_2\, u_2 - 2\pi\,\sigma\ , \tag{5}$$

i.e. two equations for the unknowns u_1, $u_2 = 2\pi\dot{R} - u_1$ and σ. By multiplying Eq. 4 by $d(\alpha_2, \alpha_1)$ and using $d(\alpha_2, \alpha_1) = 2\pi - d(\alpha_1, \alpha_2)$, we obtain:

$$\begin{aligned}
0 &= -d(\alpha_2, \alpha_1) F_s \left(1 + \frac{u_1}{V_m}\right) - \eta\, L_1 d(\alpha_2, \alpha_1) u_1 + \eta\, L_2 d(\alpha_2, \alpha_1) u_2 \\
&= -d(\alpha_2, \alpha_1) F_s \left(1 + \frac{u_1}{V_m}\right) - \eta\, L_1 d(\alpha_2, \alpha_1) u_1 + \eta\, L_2 (2\pi - d(\alpha_1, \alpha_2)) u_2 \\
&= -2\pi\sigma + \eta\, L_2 2\pi\, u_2\ ,
\end{aligned}$$

where we used Eq. 5. Hence, it holds that $u_2 = \frac{\sigma}{\eta\, L_2}$ and therefore $u_1 = 2\pi\dot{R} - \frac{\sigma}{\eta\, L_2}$ which we substitute in Eq. 4 to obtain the following simple linear equation satisfied by the contractile stress σ and the contraction rate $\dot{R}$,

$$2\pi\dot{R} = \frac{-F_s}{\frac{F_s}{V_m} + L_1\eta} + \sigma \left(\frac{1}{L_2\eta} + \frac{1}{\frac{F_s}{V_m} + L_1\eta}\right)\ .$$

From this we immediately obtain the force for isometric contraction (when $\dot{R} = 0$) and the contraction rate (when $\sigma = 0$):

$$\sigma = \frac{F_s}{1 + \frac{L_1}{L_2} + \frac{F_s/V_m}{L_2\eta}} \quad \text{and} \quad 2\pi\dot{R} = \frac{-V_m}{1 + \frac{L_1\eta V_m}{F_s}}\ . \tag{6}$$

As shown in section S1.5, this holds also true for the general model Eq. 1-Eq. 3. The ring contracts if $\dot{R} < 0$ and expands if $\dot{R} > 0$, but we call $\dot{R}$ the contraction rate in all cases to avoid confusion. Similarly, we call σ the contraction force, though the contraction corresponds to $\sigma > 0$, while $\sigma < 0$ signifies expansive force.

These equations show that the rate of change of radius is equal to free myosin velocity diminished by the crosslinking drag at the same overlap where the myosin cluster is, and by the external force on the ring mediated by the general crosslinking drag. These formulas will help to understand some of the numerical results for the general model. They suggest that crosslinking is beneficial for generating force, but only if myosin and crosslinks are partially segregated, and that crosslinking limits the rate of contraction.

S1.3 Derivation of model equations using calculus of variations

Solutions of the model equations can be considered as a generalized gradient flow. Consider a given time step Δt, an index of time steps $n = 0, 1, 2, ...$ and the time-discretized approximations of the phase space variables $\boldsymbol{\alpha}^n := (\alpha_1^n, ..., \alpha_N^n)$, $\boldsymbol{\beta}^n := (\beta_1^n, ..., \beta_M^n)$ and R^n. To avoid confusion when we compute differences within the ring topology of the cytokinesis ring, instead of the classical subtraction we will write for the difference of two angles a, b:

$$a \sim b = \mathrm{mod}(a - b + \pi, 2\pi) - \pi \in [-\pi, \pi)\ . \tag{7}$$

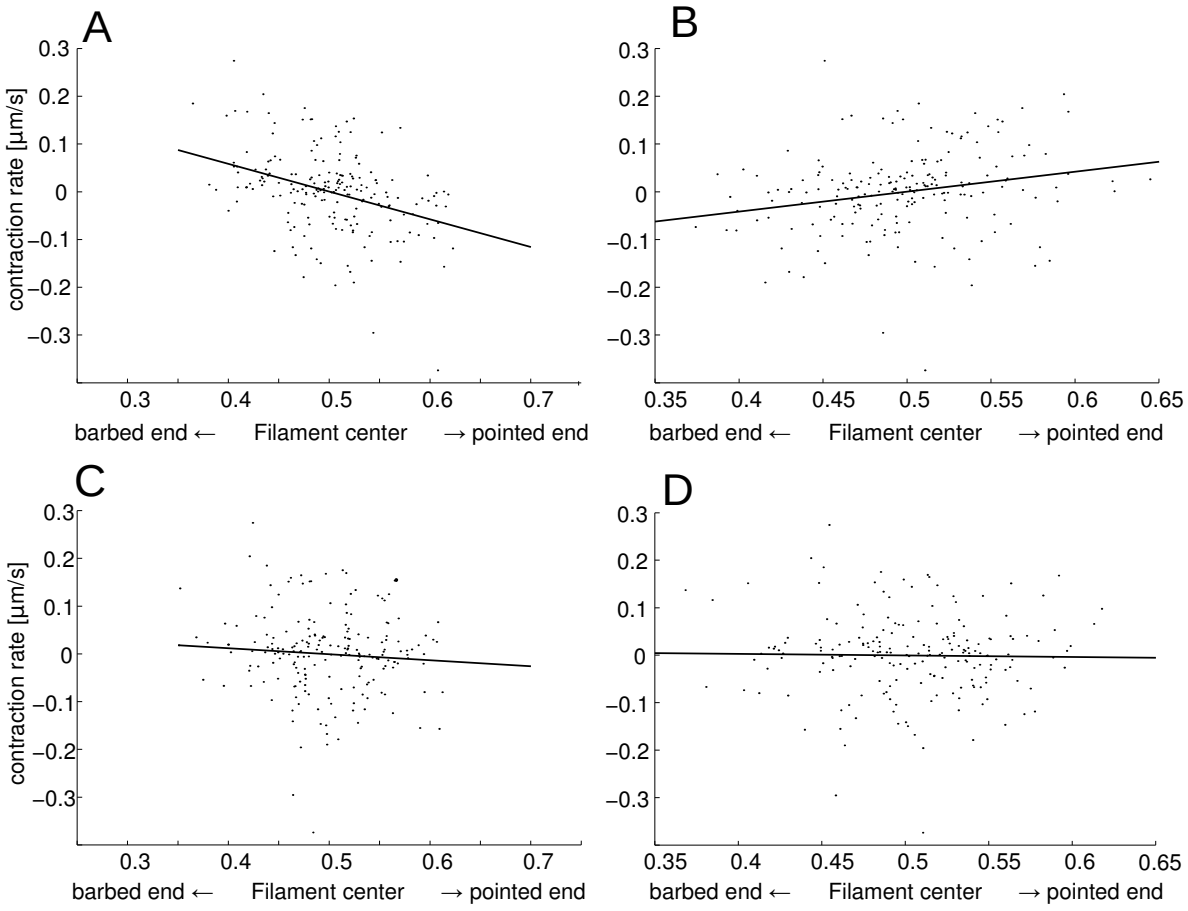

Figure S2: Extension of the numerical experiments shown in Fig. 2 C. A: See Fig. 2 C. B: The contraction rate of randomly generated actomyosin rings is also correlated to the average relative position of crosslinks treated as elastic connections between anti-parallel actin filaments (slope of the regression line is 0.24 with $p = 0.06\%$). Rings with a bias of crosslinks towards the barbed (pointed) ends of actin filaments tend to contract (expand). C: No correlation between contraction and the relative position of myosin binding sites connecting parallel actin filaments. D: No correlation between contraction and the relative position of crosslinks connecting parallel actin filaments.

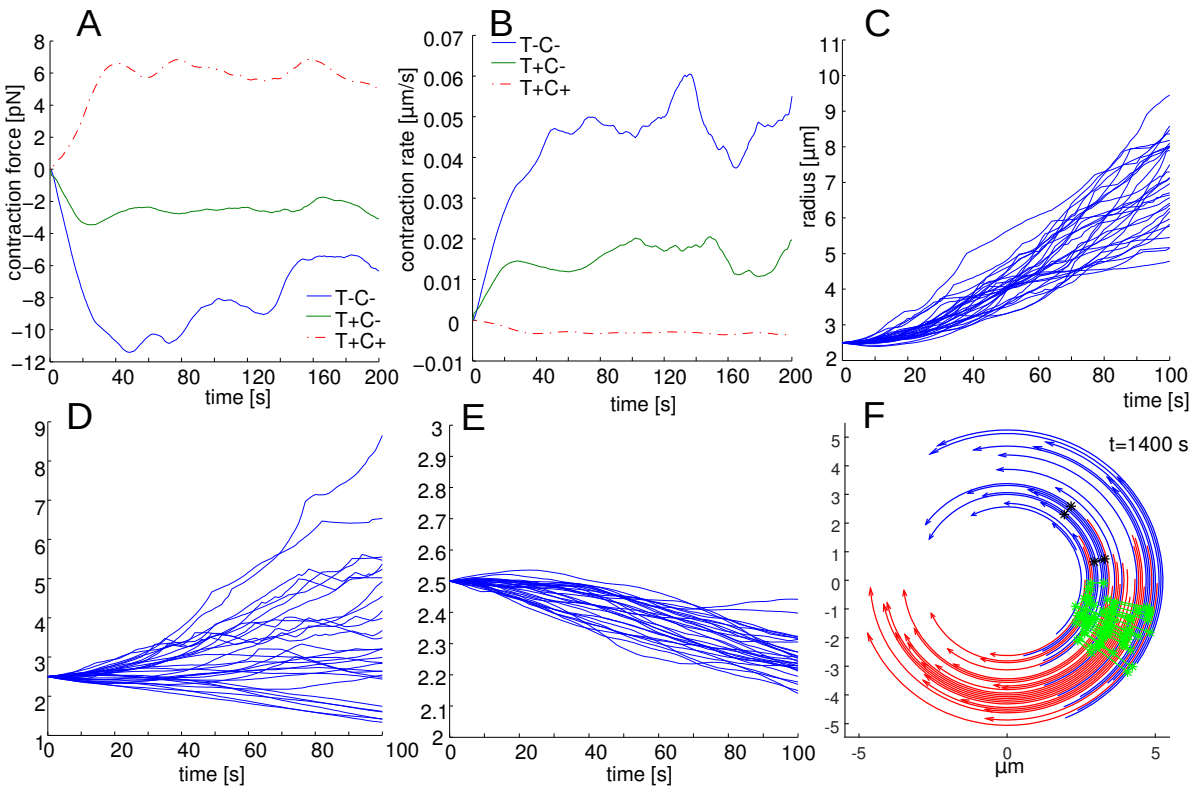

Figure S3: Comparison of contraction in three scenarios (T-C-: no treadmilling + weak crosslinking, T+C-: treadmilling + weak crosslinking and T+C+: treadmilling + strong crosslinking). In each scenario we evaluate about 20 simulation runs. A: Smoothed mean value of contraction force vs. time. B: Smoothed mean rate of contraction (dR/dt) vs. time. C: Radius vs time of the simulation runs without treadmilling and with weak crosslinking (T-C-). D: Radius vs. time of the simulation runs with treadmilling and with weak crosslinking (T+C-). E: Radius vs. time of the simulation runs with treadmilling and with strong crosslinking (T+C+). F: Snapshot at time $t = 1400$s of the simulation shown in Fig. 5 reveals a ring disruption, which happens frequently in simulations of actomyosin rings which are not contracting, e.g. under isometric conditions, after the ring has undergone polarity sorting. Rings which are free to expand typically develop actin-free gaps bordered by barbed ends. This leads to the aggregation of disconnected myosin clusters at the site of disruption. Colors are explained in the legend for Fig. 5

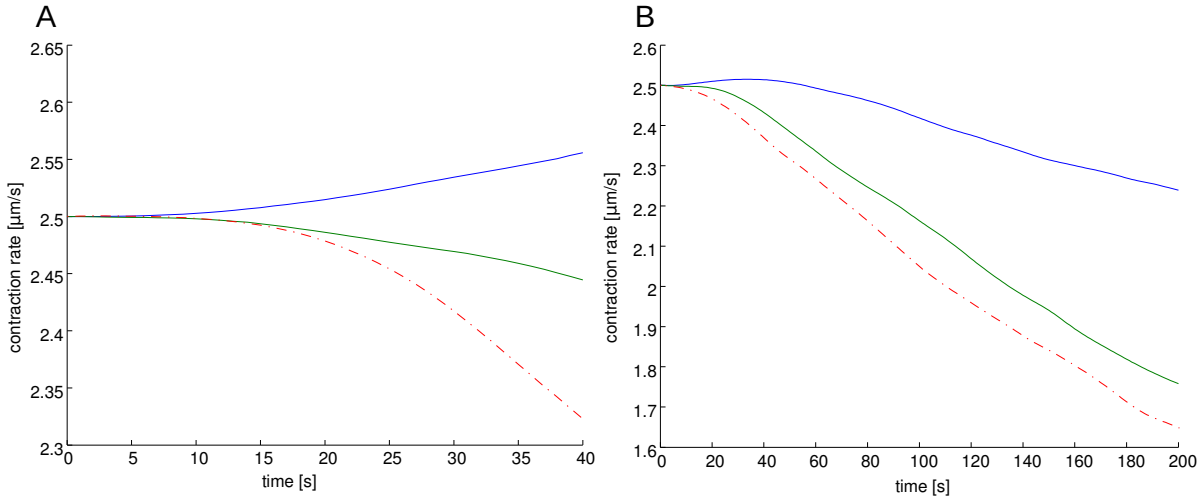

Figure S4: Contraction driven by F-actin disassembly under pressure load: Comparison of contraction dynamics in the absence of actin polymerization with pressure-induced shortening of the pointed ends of 50 % of actin filaments exposed to higher maximal pressure, at a rate of either $v_d = 0.06$ (blue), 0.12 (green) or 0.18 µm/s (red). The remaining 50 % of filaments exposed to lower maximal pressure do not disassemble. The curves represent mean values of $20 - 40$ runs. A: Rings with sufficiently fast pressure induced disassembly begin to contract soon after starting from a random configuration. However, in the absence of polymerization and nucleation this is accompanied by fast overall loss of actin. This leads to a loss of half of the original actin within 100 s (50 s, 33 s). The decrease in thickness is hardly compensated by contraction. B: Contraction in the absence of polymerizaton but with random nucleation of actin filaments at a rate which compensates for the fast disassembly of actin.

Description	Symbol	Value	Reference
Number of actin filaments	N	30	scaled down from (5) for rapid simulations
Average length of actin filaments	l	6 µm	same order of magnitude as (5)
Number of myosin clusters	M	30	scaled down from (5) for rapid simulations
Initial ring radius	R_0	2.5 µm	same order of magnitude as observed (5)
Treadmilling rate	v_p	0.1 µm s^{-1}	same order of magnitude as observed (5)
Stall force for myosin cluster	F_s	5 pN	estimated assuming that there are 20 myosin heads per cluster, 5% duty ratio of myosin motor, 5 pN stall force per head (46, 14)
Load-free myosin velocity	V_m	0.5 µm s^{-1}	see (46, 5)
Effective viscous drag due to crosslinkers	η	15 pN s µm^{-2}	see (30)

Table S1: List of reference parameters

A similar notation will be used for relative velocities within the bundle,

$$v_i \approx v_j = \frac{d}{dt}(R(\alpha_i \sim \alpha_j)) \ . \tag{8}$$

Observe that it holds that:

$$a \sim b = -(b \sim a) \quad \text{and} \quad v_i \approx v_j = -(v_j \approx v_i) \ .$$

Then, implicitly, the time-discretized version of the model equations can be derived from the variational principle:

$$(\boldsymbol{\alpha}^{n+1}, \boldsymbol{\beta}^{n+1}, R^{n+1}) = \text{argmin}\ U[\boldsymbol{\alpha}^n, \boldsymbol{\beta}^n, R^n](\boldsymbol{\alpha}, \boldsymbol{\beta}, R) \ , \tag{9}$$

which relies on the formulation of the following potential energy functional:

$$U[\boldsymbol{\alpha}^n, \boldsymbol{\beta}^n, R^n](\boldsymbol{\alpha}, \boldsymbol{\beta}, R) = -\sum_{k,i} \vartheta_{ik}\, F_s \left(n_i R(\alpha_i \sim \beta_k) - \frac{(R(\alpha_i \sim \beta_k) - R^n(\alpha_i^n \sim \beta_k^n))^2}{2\Delta t V_m} \right) + \\ + \frac{1}{2}\eta \sum_{ij} A_{ij} \frac{(R(\alpha_i \sim \alpha_j) - R^n(\alpha_i^n \sim \alpha_j^n))^2}{2\Delta t} - \sigma 2\pi R \ .$$

We solve the system Eq. 1-Eq. 3 numerically by minimizing this potential energy functional U at each computational step with respect to variables $\boldsymbol{\alpha}, \boldsymbol{\beta}, R$, knowing the values of $\boldsymbol{\alpha}^n, \boldsymbol{\beta}^n, R^n$ from the previous computational step. Values of the variables $\boldsymbol{\alpha}, \boldsymbol{\beta}, R$ minimizing $U[\boldsymbol{\alpha}^n, \boldsymbol{\beta}^n, R^n](\boldsymbol{\alpha}, \boldsymbol{\beta}, R)$ become $\boldsymbol{\alpha}^{n+1}, \boldsymbol{\beta}^{n+1}, R^{n+1}$. Note that the solutions are only defined modulo rotations around the ring.

As a consequence, it holds for the variation of U evaluated at $(\boldsymbol{\alpha}^{n+1}, \boldsymbol{\beta}^{n+1}, R^{n+1})$ that:

$$0 = \delta U[\boldsymbol{\alpha}^n, \boldsymbol{\beta}^n, R^n](\boldsymbol{\alpha}^{n+1}, \boldsymbol{\beta}^{n+1}, R^{n+1}) \cdot (\delta\boldsymbol{\alpha}, \delta\boldsymbol{\beta}, \delta R) = \\ = -\sum_{i,k} \vartheta_{ik}\, F_s \left(n_i - \frac{R^{n+1}(\alpha_i^{n+1} \sim \beta_k^{n+1}) - R^n(\alpha_i^n \sim \beta_k^n)}{\Delta t V_m} \right) \left(R^{n+1} \left(\delta\alpha_i - \delta\beta_k \right) + \delta R \left(\alpha_i^{n+1} \sim \beta_k^{n+1} \right) \right) + \\ + \frac{1}{2}\eta \sum_{ij} A_{ij} \frac{(R^{n+1}(\alpha_i^{n+1} \sim \alpha_j^{n+1}) - R^n(\alpha_i^n \sim \alpha_j^n))}{\Delta t} (R^{n+1}(\delta\alpha_i - \delta\alpha_j) + \delta R(\alpha_i^{n+1} \sim \alpha_j^{n+1})) - \sigma 2\pi \delta R \ .$$

Formally, we pass to the limit as $\Delta t \to 0$, taking into account that $v_i \approx \frac{R^{n+1}\alpha_i^{n+1} - R^n \alpha_i^n}{\Delta t}$ and $V_k \approx \frac{R^{n+1}\beta_k^{n+1} - R^n \beta_i^n}{\Delta t}$ and switch the indices i and j in the expression which involves $\delta\alpha_j$ obtaining:

$$0 = -\sum_{i,k} \vartheta_{ik}\, F_s \left(n_i - \frac{v_i \approx V_k}{V_m} \right) \left(R \left(\delta\alpha_i - \delta\beta_k \right) + \delta R \left(\alpha_i \sim \beta_k \right) \right) + \\ + \frac{1}{2}\eta \sum_{ij} A_{ij} (v_i \approx v_j)(2R\delta\alpha_i + \delta R(\alpha_i \sim \alpha_j)) - \sigma 2\pi \delta R \ .$$

Collecting the coefficients in front of $\delta\alpha_i$, $\delta\beta_k$ and δR, we obtain the system of equations:

$$0 = -\sum_k \vartheta_{ik}\, F_s \left(n_i - \frac{v_i \approx V_k}{V_m} \right) + \sum_j \eta\, A_{ij} \left(v_i \approx v_j \right) \ , \tag{10}$$

$$0 = \sum_i \vartheta_{ik}\, F_s \left(n_i - \frac{v_i \approx V_k}{V_m} \right) \ , \tag{11}$$

$$2\pi\sigma = -\sum_{i,k} \vartheta_{ik}\, F_s(\alpha_i \sim \beta_k) \left(n_i - \frac{v_i \approx V_k}{V_m} \right) + \frac{1}{2} \sum_{i,j} \eta\, A_{ij} (\alpha_i \sim \alpha_j) \left(v_i \approx v_j \right) \ . \tag{12}$$

The contraction force can be introduced as the force per cross-section of the ring, which does not vary from one cross-section to another. Here we analyze whether this notion can be applied in our model Eq. 10-Eq. 12.

Recall that $\alpha_i \sim \alpha_j = \alpha_i - \alpha_j + \tau_{ij} 2\pi$ and $\alpha_i \sim \beta_k = \alpha_i - \beta_k + \bar{\tau}_{ik} 2\pi$ where $\tau_{ij}, \bar{\tau}_{ik} \in \mathbb{Z}$. Pick one cross-section located at the angle γ. Without loss of generality assume that all angles $\alpha_1, ..., \alpha_N$ and $\beta_1, ..., \beta_M$ are written as real numbers in the interval $[\gamma, \gamma + 2\pi)$. Then Eq. 12 reads:

$$2\pi\sigma = -\sum_{i,k} \vartheta_{ik}\, F_s(\alpha_i - \beta_k + \bar{\tau}_{ik} 2\pi) \left(n_i - \frac{v_i \approx V_k}{V_m} \right) + \frac{1}{2} \sum_{i,j} \eta\, A_{ij} (\alpha_i - \alpha_j + \tau_{ij} 2\pi)\, (v_i \approx v_j)$$

and simplifies, using Eq. 10 and Eq. 11, to:

$$\sigma = -\sum_{i,k} \vartheta_{ik}\, F_s\, \bar{\tau}_{ik} \left(n_i - \frac{v_i \approx V_k}{V_m} \right) + \frac{1}{2} \sum_{i,j} \eta\, A_{ij}\, \tau_{ij}\, (v_i \approx v_j) \ . \tag{13}$$

which confirms system Eq. 1-Eq. 3 in the main text. Only those coefficients τ_{ij} and $\bar{\tau}_{ik}$ are different from zero and equal to ± 1 for which indices i and j correspond to two actin filaments, or one actin and one myosin filament, which, first, interact, and second, cross the cross-section located at γ. Specifically, in the case of two actin filaments, the two angular positions α_i and α_j have to be on opposite sides of the cross-section such that $\alpha_i \sim \alpha_j = \alpha_i - \alpha_j \pm 2\pi$. The same has to hold for the angular positions of a pair of interacting actin and myosin filaments to be taken into account.

Hence, according to Eq. 13, the contraction force σ can be computed by summing up all the forces transmitted by crosslinks and myosin-actin interactions through a given specific cross-section. For the interpretation of the original equation Eq. 3, this means that the differences of angles $\alpha_i \sim \beta_k$ and $\alpha_i \sim \alpha_j$ do not play the role of coefficients measuring the contribution of single myosin filaments or crosslinks to overall stress. Instead, these factors serve as placeholders for either ± 1, or zero, restricting that sum to the contributions at a fixed position along the ring.

S1.4 Cross-linkers as elastic springs

We derive implicitly time-discretized model equations from the variational principle Eq. 9 with the modified potential energy functional,

$$U[\boldsymbol{\alpha}^n, \boldsymbol{\beta}^n, R^n](\boldsymbol{\alpha}, \boldsymbol{\beta}, R) := -\sum_{k,i} \vartheta_{ik}\, F_s \left(n_i R(\alpha_i \sim \beta_k) - \frac{(R(\alpha_i \sim \beta_k) - R^n(\alpha_i^n \sim \beta_k^n))^2}{2\Delta t V_m} \right) + \\ + \frac{1}{2} \kappa_{\mathrm{cl}} \sum_{ij} \psi_{ij} \frac{(R(\alpha_i \sim \alpha_j) - R^0(\alpha_i^0 \sim \alpha_j^0))^2}{2} - \sigma 2\pi R \ .$$

by replacing the drag friction between actin filaments by a finite number of M_{cl} crosslinkers, each modeled as an elastic spring that connects specific binding sites on specific actin filaments and which is characterized by the spring coefficient κ_{cl}. To compute one time step we assume that crosslinkers are totally relaxed initially, and replace expression $\eta A_{ij}/\Delta t$ by expression $\kappa_{\mathrm{cl}}\, \psi_{ij}$. Here ψ_{ij} represents the number of crosslinkers connecting the filaments with indices i and j, and the elastic coefficient of crosslinkers is chosen to be $\kappa_{\mathrm{cl}} = 1000\,\mathrm{pN\,\mu m^{-1}}$.

The model equations in this case have the form:

$$\begin{aligned}
0 &= -\sum_k \vartheta_{ik}\, F_s \left(n_i - \frac{v_i \approx V_k}{V_m} \right) + \\
&\qquad + \sum_j \kappa_{\mathrm{cl}}\, \psi_{ij} \left((R^{n+1}(\alpha_i^{n+1} \sim \alpha_j^{n+1}) - R^0(\alpha_i^0 \sim \alpha_j^0)) \right) \ , \\
0 &= \sum_i \vartheta_{ik}\, F_s \left(n_i - \frac{v_i \approx V_k}{V_m} \right) \ , \\
2\pi\sigma &= -\sum_{i,k} \vartheta_{ik}\, F_s(\alpha_i \sim \beta_k) \left(n_i - \frac{v_i \approx V_k}{V_m} \right) + \\
&\qquad + \frac{1}{2} \sum_{i,j} \kappa_{\mathrm{cl}}\, \psi_{ij}(\alpha_i \sim \alpha_j) \left((R^{n+1}(\alpha_i^{n+1} \sim \alpha_j^{n+1}) - R^0(\alpha_i^0 \sim \alpha_j^0)) \right) \ .
\end{aligned}$$

S1.5 Linear force-velocity relation between the contraction rate $\dot{R}$ and the contraction force σ.

Here we show that the contraction force σ and the contraction rate $\dot{R}$ satisfy a relation of the type $a\sigma = b\dot{R} + c$ for three constants a, b, c. To this end, we substitute:

$$\begin{aligned}
v_i \approx v_j &= \frac{d}{dt} \left(R\left(\alpha_i \sim \alpha_j\right) = \dot{R}(\alpha_i \sim \alpha_j) + R(t)(\dot{\alpha}_i - \dot{\alpha}_j) \right. \\
v_i \approx V_k &= \frac{d}{dt} \left(R\left(\alpha_i \sim \beta_k\right) = \dot{R}(\alpha_i \sim \beta_k) + R(t)(\dot{\alpha}_i - \dot{\beta}_k) \right.
\end{aligned} \tag{14}$$

into the model equations. We write the resulting system as:

$$\begin{aligned}
F_s n_i \sum_k \vartheta_{ik} - \dot{R} \left(\frac{F_s}{V_m} \sum_k \vartheta_{ik} \left(\alpha_i \sim \beta_k\right) + \sum_j \eta\, A_{ij} (\alpha_i \sim \alpha_j) \right) = \qquad (15) \\
= R(t) \left(\frac{F_s}{V_m} \sum_k \vartheta_{ik} (\dot{\alpha}_i - \dot{\beta}_k) + \sum_j \eta\, A_{ij} \left(\dot{\alpha}_i - \dot{\alpha}_j\right) \right) \ , \\
-\sum_i \vartheta_{ik}\, F_s n_i + \dot{R} \frac{F_s}{V_m} \sum_i \vartheta_{ik} (\alpha_i \sim \beta_k) = \qquad (16) \\
= -\frac{F_s}{V_m} R(t) \sum_i \vartheta_{ik} (\dot{\alpha}_i - \dot{\beta}_k) \ , \\
2\pi\sigma = -\sum_{i,k} \vartheta_{ik}\, F_s(\alpha_i \sim \beta_k) \left(n_i - \frac{1}{V_m} \left(\dot{R}(\alpha_i \sim \beta_k) + R(t)(\dot{\alpha}_i - \dot{\beta}_k) \right) \right) + \qquad (17) \\
+ \frac{1}{2} \sum_{i,j} \eta\, A_{ij} (\alpha_i \sim \alpha_j) \left(\dot{R}(\alpha_i \sim \alpha_j) + R(t)(\dot{\alpha}_i - \dot{\alpha}_j) \right) \ .
\end{aligned}$$

We treat the subsystem Eq. 15-Eq. 16 as a linear system with respect to $(\dot{\alpha}_1, ..., \dot{\alpha}_N, \dot{\beta}_1, ..., \dot{\beta}_k)$. Observe that due to the lack of friction against the immobile exterior of the ring, solution vectors are not unique. Families of solutions are generated by adding arbitrary constants since the system Eq. 15-Eq. 16 only contains relative velocities. For simplicity, we assume that there only exists one such family of solutions and we infer that any given representative of that family can be written as $(\dot{\alpha}_1, ..., \dot{\alpha}_N, \dot{\beta}_1, ..., \dot{\beta}_k) = \mathbf{c_1} + \dot{R}\mathbf{c_2}$ for two vectors $\mathbf{c_1}, \mathbf{c_2} \in \mathbb{R}^{N+M}$.

We substitute that solution into Eq. 17, which only contains relative velocities too and which is therefore invariant with respect to adding a constant rotation angle. As a consequence, equation Eq. 17

adopts the structure $2\pi\sigma = b\dot{R} + c$ where b and c are constants independent of the external force σ and the contraction rate $\dot{R}$.

The linearity of the force-velocity relation is a very useful result because it can be used to predict the ring radius as a function of time if we know the outside pressure on the ring as a function of either time, or radius. This would require modeling of cellular cytoplasm and cortex, as well as of mechanical connections between the ring and the rest of the cell.

S1.6 Mechanics of three overlapping actin filaments

To illustrate how the mathematical model Eq. 1-Eq. 3 works from the point of view of elementary mechanics, we consider the special case of an actomyosin ring consisting of just three actin filaments and one myosin cluster (Fig. S1 B). We derive explicit expressions for the velocities and contractile stress in the ring and illustrate the fact that the contractile stress σ given by Eq. 3 does not vary in space and corresponds to the sum of mechanical forces across an arbitrary cross-section of the ring. For simplicity, we will analyze the isometric case only, $\dot{R} = 0$.

In the following computations, all angles are within interval $[0, 2\pi)$. The polarities of the actin filaments shown in Fig. S1 B are $n_3 = -n_1 = -n_2 = 1$ and, following the notation introduced in Eq. 7, we have $\alpha_1 \sim \alpha_2 = \alpha_1 - \alpha_2$, $\alpha_1 \sim \alpha_3 = \alpha_1 - \alpha_3$ as well as $\alpha_2 \sim \alpha_3 = \alpha_2 - \alpha_3 + 2\pi$. Furthermore we have $\alpha_1 \sim \beta_1 = \alpha_1 - \beta_1$ and $\alpha_2 \sim \beta_1 = \alpha_2 - \beta_1 + 2\pi$.

We write $v_i = R\frac{d}{dt}\alpha_i$ and $V_1 = R\frac{d}{dt}\beta_1$. The relative velocities Eq. 8 are thus given by $v_1 \approx v_2 = v_1 - v_2$, $v_1 \approx v_3 = v_1 - v_3$, $v_2 \approx v_3 = v_2 - v_3$ as well as $v_1 \approx V_1 = v_1 - V_1$, $v_2 \approx V_1 = v_2 - V_1$.

Eq. 11 for the velocity of the myosin cluster is: $0 = F_s\left(-1 - \frac{v_2 \approx V_1}{V_m}\right) + F_s\left(1 - \frac{v_3 \approx V_1}{V_m}\right)$ and it implies that

$$V_1 = \frac{v_2 + v_3}{2} \ .$$

The equations for the velocities of actin filaments Eq. 1, read:

$$0 = \eta\, A_{12}\,(v_1 - v_2) + \eta\, A_{13}\,(v_1 - v_3) \ , \tag{18}$$

$$0 = -F_s\left(-1 - \frac{v_2 - v_3}{2V_m}\right) + \eta\, A_{12}\,(v_2 - v_1) + \eta\, A_{23}\,(v_2 - v_3) \ , \tag{19}$$

$$0 = -F_s\left(1 - \frac{v_3 - v_2}{2V_m}\right) + \eta\, A_{13}\,(v_3 - v_1) + \eta\, A_{23}\,(v_3 - v_2) \ . \tag{20}$$

Note that Eq. 18 is the sum of Eq. 19 and Eq. 20 reflecting the fact that solutions are invariant with respect to rotations. We omit Eq. 20, fix $v_1 = 0$ and obtain from Eq. 18:

$$v_3 = -A_{12}/A_{13} v_2 \ , \tag{21}$$

which allows to write Eq. 19 as:

$$-F_s = \left(\eta\, A_{12} + (\eta\, A_{23} + F_s \frac{1}{2V_m})\,(1 + A_{12}/A_{13})\right) v_2 \ .$$

This gives us all filament velocities:

$$\begin{pmatrix} v_1 \\ v_2 \\ v_3 \end{pmatrix} = \frac{F_s}{\left(\eta\, A_{12} + (\eta\, A_{23} + F_s \frac{1}{2V_m})\,(1 + A_{12}/A_{13})\right)} \begin{pmatrix} 0 \\ -1 \\ A_{12}/A_{13} \end{pmatrix} \ .$$

The contraction force in this case is given by the general equation Eq. 3, which, in the present example, has the form:

$$\sigma = -F_s\left(-1 - \frac{v_2 - v_3}{2V_m}\right) + \eta\, A_{23}\,(v_2 - v_3) \ . \tag{22}$$

Note that subtracting Eq. 19 from Eq. 22, we obtain a much simpler expression for the contractile stress:

$$\sigma = \eta\, A_{12}\,(v_1 - v_2)\ . \tag{23}$$

Another simple expression for the contractile stress can be obtained if we compare Eq. 23 with Eq. 21:

$$\sigma = \eta A_{13} v_3 = \eta A_{13}(v_3 - v_1)\ . \tag{24}$$

Observe that if we choose any cross-section of the ring crossing only one filament in the ring, no matter which one, then from Fig. S1 B, it is clear that the stress acting at the crossed point on the filament is equal to the drag force from either the overlap between filaments 1 and 2, or between filaments 1 and 3. Equations Eq. 23 and Eq. 24 give respective forces, but we just showed that these two forces are the same, and also equal to the contractile stress given by the general equation of the model!

Moreover, if we chose a more complex example and have the cross-section bisecting both filaments 1 and 3, as shown in Fig. S1 B, then the intrafilamentous stress in filament 1 there is equal to $\eta y(v_3 - v_1)$, the stress in filament 3 is equal to $\eta x(v_3 - v_1)$, and the total stress is $\eta(x + y)(v_3 - v_1) = \eta A_{13}(v_3 - v_1)$, again the same contraction force, regardless of where exactly the cross-section is. Derivation for cross-sections bisecting the region of the overlaps of filaments 1 and 2 is exactly the same; for cross-sections bisecting the region of the overlaps of filaments 2 and 3, it is slightly more complex because of the myosin cluster there, but the result is, again, the same.

S1.7 Compression-induced actin disassembly increases contractility

Compression can develop in actin filaments if, for example, a crosslink holds the pointed end fixed, while a myosin cluster slides respective barbed end toward the pointed end. We investigate the effect of such compression assuming the compression-induced severing and disassembly in the following way. At every discrete time step, we compute the pressure (compression is positive pressure, tension is negative one) profile along any actin filament taking into account distributed forces from crosslinks and point forces from myosin. Then, for every actin filament, we determine the maximal pressure along its length which is never negative since the filament tips are always force free. We select 50% of all actin filaments with highest peak pressure and increase their depolymerization rate by 0.05 µm/s while the depolymerization rates of the remaining filaments is decreased by the same value. The polymerization rate of 0.1 µm/s for all barbed ends does not vary, which conserves the amount of F-actin. The simulation indicates that increased disassembly under pressure leads to an even stronger positional bias of myosin sites towards the pointed ends of actin filaments leading to an increase in contraction force and contraction rate, as compared to actomyosin rings with uniform rates of actin disassembly (Fig. 2 F).

Thus, the mechanical asymmetry assists the contraction in the presence of treadmilling. To test whether compression-induced severing can also drive contraction in the absence of actin polymerization, we simulated random actin arrays based on the reference parameter set as listed in Table S1. The rate of polymerization, however, is set to zero, and the rate of disassembly is given by a positive constant if a specific actin filament is among the 50 % of filaments under higher pressure, otherwise the rate of disassembly is set to zero. In Fig. S4 in the Supporting Material we compare the mean values of the radii for three different rates of pressure-induced actin disassembly. Indeed, the faster the disassembly rate is, the faster the ring contracts. However, due to the fast rate of disassembly, F-actin is released from the ring much faster than the rings typically contract causing the F-actin concentration to decrease: a ring in the simulations dissolves in approximately 100 s, while contractile rings in experiments take hundreds of seconds to contract (6).

Therefore, we explored the possibility that random nucleation of actin filaments replenishes the ring by randomly adding filaments at the rate such that the initial number of filaments is roughly conserved. Furthermore, we assumed that short filaments of a length smaller than 1 µm depolymerize irrespective of the pressure they are exposed to, in order for the ring not to get overloaded with short filaments. As a result (Fig. S4 B), we confirmed that compression-triggered actin filament severing in combination with F-actin nucleation can maintain contractility over longer periods of time.

Movie S1 Contraction of a random actomyosin ring of initial radius $R = 5\,\mu\text{m}$ with initially 90 actin filaments and 90 myosin clusters. Actin filaments are removed at the rate which approximately maintains a constant actin concentration during contraction. Note that the ring in the movie occasionally bounces to a larger size, but this is not an actual size increase: at these moments we simply change the length scale to represent the shrinking ring in detail. Actin filaments with their pointed ends marked by an arrow in anti-clockwise (clockwise) direction are blue (red). Stars on actin filaments represent myosin binding sites and myosin clusters connecting them are shown as transversal lines. These are drawn in green (black) if the connected actin filaments are anti-parallel (parallel).

Movie S2 Contraction of a random actomyosin ring of initial radius $R = 5\,\mu\text{m}$ with 90 actin filaments and initially 90 myosin clusters. Actin filaments shorten at the rate which approximately maintains a constant actin concentration during contraction. Myosin is also released during contraction at the rate which approximately maintains a constant myosin concentration during contraction. Note that the ring in the movie occasionally bounces to a larger size, but this is not an actual size increase: at these moments we simply change the length scale to represent the shrinking ring in detail. Actin filaments with their pointed ends marked by an arrow in anti-clockwise (clockwise) direction are blue (red). Stars on actin filaments represent myosin binding sites and myosin clusters connecting them are shown as transversal lines. These are drawn in green (black) if the connected actin filaments are anti-parallel (parallel).

Movie S3 Contraction force generation in isometric actomyosin ring of radius $R = 2.5\,\mu\text{m}$ with 45 actin filaments and 45 myosin clusters. The degree of polarity sorting increases as anti-clockwise and clockwise actin filaments gradually concentrate at the same position while they keep treadmilling around the ring. Actin filaments with their pointed ends marked by an arrow in anti-clockwise (clockwise) direction are blue (red). Stars on actin filaments represent myosin binding sites and myosin clusters connecting them are shown as transversal lines. These are drawn in green (black) if the connected actin filaments are anti-parallel (parallel). Blue stars represent myosin filaments detached from actin filaments. The polarity graph (top right) shows the sum of anti-clockwise filaments counted as $+1$ and clockwise filaments counted as -1. Over time, the amplitude of polarity fluctuations increases illustrating the tendency of the ring to polarize. In synchrony with periodic polarity increase, the distribution of myosin clusters becomes increasingly inhomogeneous as shown in the histogram (bottom right), with greater fraction of myosin accumulating to fewer spots.